Doping evolution of antiferromagnetic order and structural distortion in LaFeAsO$_{1-x}$F$_x$

Q. Huang,[1] Jun Zhao,[2] J. W. Lynn,[1] G. F. Chen,[3] J. L. Luo,[3] N. L. Wang,[3] and Pengcheng Dai[2,4,*]

[1]*NIST Center for Neutron Research, National Institute of Standards and Technology, Gaithersburg, Maryland 20899-6102, USA*
[2]*Department of Physics and Astronomy, The University of Tennessee, Knoxville, Tennessee 37996-1200, USA*
[3]*Beijing National Laboratory for Condensed Matter Physics, Institute of Physics, Chinese Academy of Sciences, P.O. Box 603, Beijing 100080, People's Republic of China*
[4]*Neutron Scattering Science Division, Oak Ridge National Laboratory, Oak Ridge, Tennessee 37831-6393, USA*

We use neutron scattering to study the structural distortion and antiferromagnetic (AFM) order in LaFeAsO$_{1-x}$F$_x$ as the system is doped with fluorine (F) to induce superconductivity. In the undoped state, LaFeAsO exhibits a structural distortion, changing the symmetry from tetragonal (space group $P4/nmm$) to orthorhombic (space group $Cmma$) at 155 K, and then followed by an AFM order at 137 K. Doping the system with F gradually decreases the structural distortion temperature, but suppresses the long range AFM order before the emergence of superconductivity. Therefore, while superconductivity in these Fe oxypnictides can survive in either the tetragonal or the orthorhombic crystal structure, it competes directly with static AFM order.

I. INTRODUCTION

A determination of the phase diagram in the FeAs-based RFeAsO$_{1-x}$F$_x$ (where R=La,Nd,Sm,Pr,…) family of high-transition temperature (high-T_c) superconductors[1–6] is the first step necessary for a comprehensive understanding of their electronic properties. The parent compounds of these FeAs-based materials are nonsuperconducting semimetals. When cooling down from room temperature, RFeAsO first exhibits a structural phase transition, changing the crystal symmetry from tetragonal (space group $P4/nmm$) to orthorhombic (space group $Cmma$), and then orders antiferromagnetically with a spin structure as shown in Figs. 1(a) and 1(b).[7–13] While earlier work had shown that superconductivity induced by F doping suppresses both the structural phase transition and static antiferromagnetic (AFM) order,[7] how this process occurs in RFeAsO$_{1-x}$F$_x$ as a function of F doping is still unclear. For example, in a systematic study of the F-doping dependence of the structural and magnetic phase diagram of CeFeAsO$_{1-x}$F$_x$, Zhao *et al.*[8] found that the Fe AFM order disappears before the appearance of superconductivity. However, it was not clear whether the orthorhombic structural distortion in the undoped compound is still present in the underdoped superconducting materials. On the other hand, while systematic x-ray diffraction experiments on SmFeAsO$_{1-x}$F$_x$ reveal that orthorhombic symmetry is present in the underdoped superconductors, there are no neutron-scattering experiments to directly probe the AFM phase boundary in these materials.[14] Finally, recent μSR, transport, and Mössbauer experiments on the phase diagram of LaFeAsO$_{1-x}$F$_x$ suggest a first-order-like phase transition between the AFM and superconducting phases.[15] Furthermore, these authors argue that the tetragonal to orthorhombic structural phase transition is associated with the doping-induced AFM to superconductivity phase transition, a result clearly inconsistent with Ref. 14.

The difficulty in obtaining a comprehensive phase diagram of RFeAsO$_{1-x}$F$_x$ stems from the fact that various local

probes such as μSR and Mössbauer can detect magnetic long-range order but are insensitive to the structural distortion.[15] On the other hand, x-ray scattering is sensitive to structural distortion but does not directly probe the AFM order. Neutron scattering is capable of detecting both structural and magnetic order, but requires large sample masses and therefore has only been done for a limited doping range in CeFeAsO$_{1-x}$F$_x$.[8] In this paper, we present a systematic neutron-scattering investigation of LaFeAsO$_{1-x}$F$_x$ that complements earlier work on this system.[7,11,15] Our data reveal that the orthorhombic structural distortion extends beyond the AFM phase and coexists with superconductivity, whereas there is no evidence of static long-range AFM order coexisting with superconductivity.

II. EXPERIMENTAL RESULTS AND DISCUSSIONS

We use neutron diffraction to study the structural and magnetic phase transitions in polycrystalline samples of LaFeAsO$_{1-x}$F$_x$ with fluorine doping x=0,0.03,0.05, and 0.08. Our experiments were performed on the BT-1 high resolution powder diffractometer and BT-7 triple axis spectrometer at the NIST Center for Neutron Research, Gaithersburg, Maryland. The BT-1 diffractometer has a Ge(3,1,1) monochromator and an incident wavelength of λ=2.0785 Å. Collimators with horizontal divergences of 15′, 20′, and 7′ full width at half maximum (FWHM) were used before and after the monochromator, and after the sample, respectively. BT-7 has a PG(0,0,2) (pyrolytic graphite) monochromator with an incident-beam wavelength of λ=2.359 Å. A PG filter was placed in the incident-beam path to eliminate $\lambda/2$.[7,8] The collimations are 50′ FWHM before the sample and 80′ radial collimator between the sample and a position sensitive detector that covered an angular range of approximately 5°. The polycrystalline samples of LaFeAsO$_{1-x}$F$_x$ with x=0,0.03,0.05, and 0.08 were prepared by the solid-state reaction using LaAs, Fe$_2$O$_3$, Fe, and LaF$_3$ as starting materials, with the detailed preparation method described in Ref. 6. We
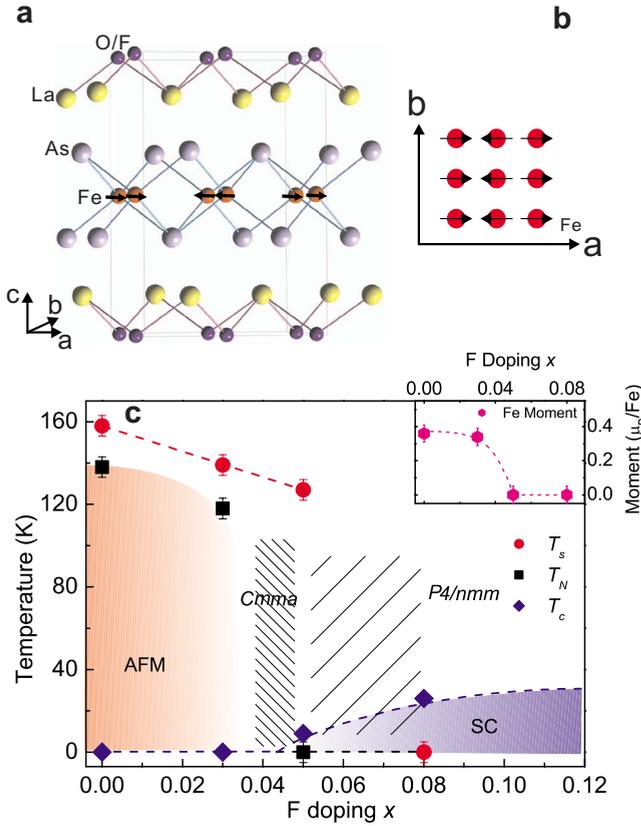
FIG. 1. (Color online) (a) The Fe spin ordering in the LaFeAsO chemical unit cell. (b) The Fe magnetic unit cell of LaFeAsO in the Fe-As plane. The Fe moments lie in the *a-b* plane along the *a* axis and form an antiferromagnetic collinear spin structure similar to $BaFe_2As_2$, $SrFe_2As_2$, and $CaFe_2As_2$ (Refs. 7–10) (c) The structural and magnetic phase diagram determined from our neutron measurements on $LaFeAsO_{1-x}F_x$ with $x=0, 0.03, 0.05, 0.08$. The red circles indicate the onset temperature of the $P4/nmm$ to $Cmma$ phase transition. The black squares designate the Néel temperatures of Fe as determined from neutron measurements in Fig. 3. The superconducting transition temperatures T_c for $x=0.05, 0.08$ are determined from susceptibility measurements. The AFM to superconducting phase transition happens between $x=0.03$ and 0.05. The inset in (d) shows the F doping dependence of the Fe moment as determined from the intensity of the $(1,0,3)_M$ magnetic peak at 4 K.

checked the superconducting properties of each $LaFeAsO_{1-x}F_x$ sample using a superconducting quantum interference device (SQUID) magnetometer and found that the $x=0, 0.03$ samples are nonsuperconducting, while the $x=0.05$ and 0.08 samples are 8 and 26 K superconductors, respectively. The fluorine-doping levels are nominal, and should be close to the actual electron-doping level at these concentrations.

Figures 1(a) and 1(b) show the Fe spin structure within the FeAs layer as determined from previous neutron-scattering work on *R*FeAsO (Refs. 7, 8, and 11) and $(Ba,Sr,Ca)Fe_2As_2$.[9,10,13] Figure 1(c) summarizes the electronic phase diagram of $LaFeAsO_{1-x}F_x$ determined from our measurements. Our data are consistent with previous neutron scattering[7] and results from local probes such as μSR and [57]Fe Mössbauer spectroscopy,[15] and indicates that long-range
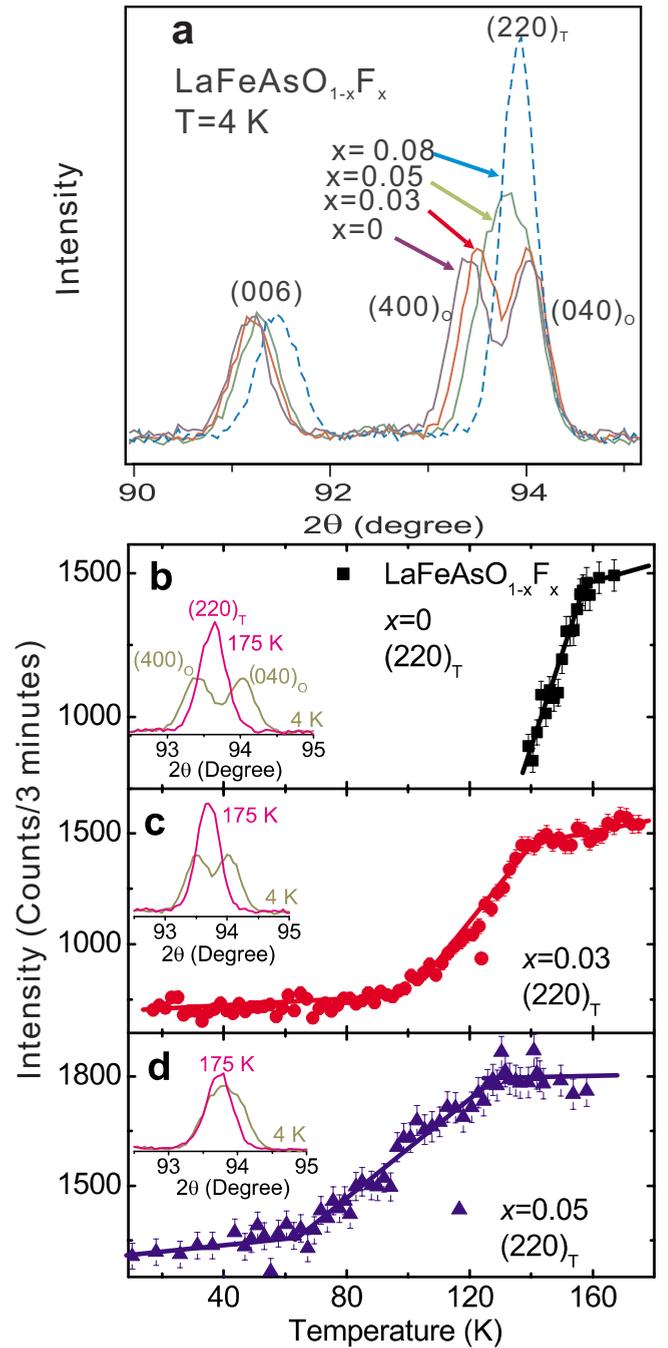

FIG. 2. (Color online) Dependence of the low-temperature crystal structure of $LaFeAsO_{1-x}F_x$ as a function of F-doping *x*. (a) 2θ scans, showing the reduction of the orthorhombic lattice distortion with increasing F doping. The $(2,2,0)$ peak for $x=0.05$ is clearly broader than the resolution. [(b)–(d)] Temperature dependence of the $(2,2,0)_T$ (T denotes tetragonal) nuclear reflection indicative of a structural phase transition for various *x* (Ref. 7). The temperature of the tetragonal to orthorhombic lattice distortion reduces with increasing *x*. The insets show the $(2,2,0)_T$ reflection above and below the transition temperatures.

AFM order disappears as a function of doping before superconductivity is present. On the other hand, we find direct evidence for the orthorhombic structural distortion in the underdoped superconducting $LaFeAsO_{1-x}F_x$, indicating that the
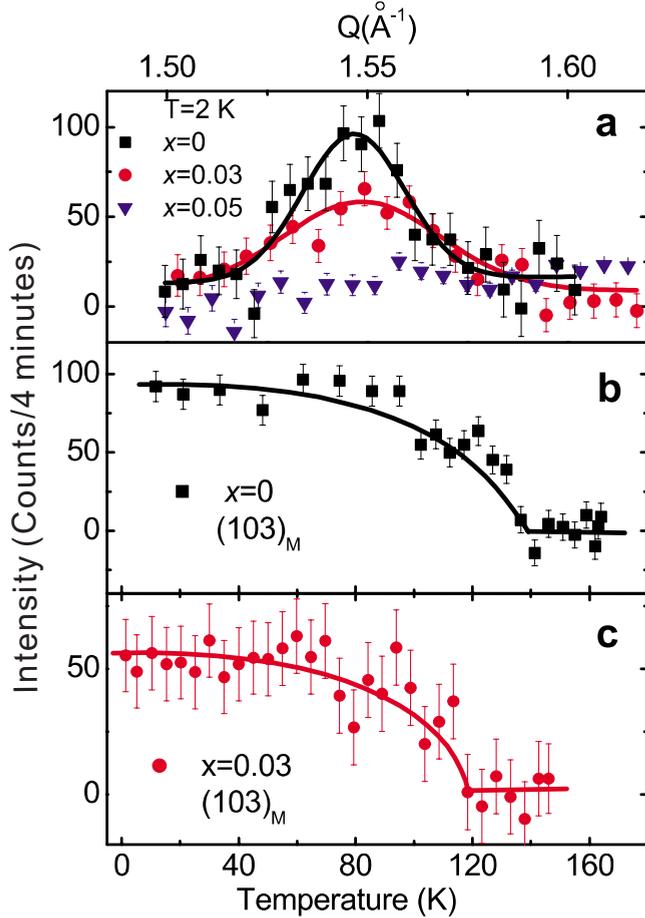
FIG. 3. (Color online) (a) Wave vector dependence of the AFM ordering peak (1,0,3) for $x=0,0.03,0.05$ at 2 K. The intensity of scattering is normalized to the nuclear Bragg peaks and can be compared directly. (b) and (c) Temperature dependence of the magnetic scattering for $x=0,0.03$, respectively.

TABLE I. Refined crystal structure parameters of LaFeAsO$_{1-x}$F$_x$ with $x=0$ at 175 K ($R_p=5.24\%$, $w_{Rp}=6.62\%$, $\chi^2=0.9825$), and $x=0.08$ at 10 K ($R_p=5.05\%$, $w_{Rp}=6.6\%$, $\chi^2=0.9273$). Space group: $P4/nmm$. LaFeAsO, $a=4.03007(9)$, $c=8.7368(2)$ Å; LaFeAsO$_{0.92}$F$_{0.08}$, $a=4.02005(4)$, $c=8.7032(1)$ Å.

Atom	site	X	y	$z(x=0)$	$z(x=0.08)$
La	$2c$	$\frac{1}{4}$	$\frac{1}{4}$	0.1417(3)	0.1450(3)
Fe	$2b$	$\frac{3}{4}$	$\frac{1}{4}$	$\frac{1}{2}$	$\frac{1}{2}$
As	$2c$	$\frac{1}{4}$	$\frac{1}{4}$	0.6507(4)	0.6520(3)
O	$2a$	$\frac{3}{4}$	$\frac{1}{4}$	0	0

going through the tetragonal to orthorhombic symmetry change. Figures 2(b)–2(d) show that this is indeed the case, where the tetragonal to orthorhombic symmetry change temperature reduces systematically as a function of increasing F doping.

Figure 3 summarizes the F-doping dependence of the AFM Bragg peak and magnetic order parameter. μSR measurements on LaFeAsO$_{1-x}$F$_x$ with $x=0,0.03$ (Ref. 16) confirmed that the undoped parent LaFeAsO compound has static AFM order, but the 3% F doping might induce an incommensurate/stripe-like AFM magnetic order. To determine the F-doping dependence of the AFM order, we probed the (1,0,3) magnetic peak. Figure 3(a) plots the wave vector dependence of the (1,0,3) at 2 K. When 3% F is introduced, the (1,0,3) peak becomes weaker and broader. The broadening can be interpreted as a reduction in the Fe spin-spin correlation length from 208 ± 28 Å for $x=0$ to 139 ± 33 Å for $x=0.03$, with the scattering still being commensurate and centered at (1,0,3) for both materials. This broadening is somewhat different from the doping-dependent magnetic scattering for CeFeAsO$_{1-x}$F$_x$,[8] where the magnetic peaks at finite F dopings were always resolution limited. This suggests that the broadening might be interpreted as originating from incommensurate AFM magnetic order, with an incommensurability that cannot be resolved. Future experiments on single crystals should be able to resolve this issue. On further increasing the F doping to $x=0.05$, where superconductivity with $T_c=8$ K is induced, the (1,0,3) static AFM ordering peak is no longer observable [Fig. 3(a)]. Therefore, while the orthorhombic lattice distortion extends to samples with bulk superconductivity, static AFM order does not coexist with superconductivity within the accuracy of our measurements.[17]

Figures 3(b) and 3(c) show the temperature dependence of the (1,0,3) peak intensity. Consistent with previous neutron scattering[7,11] and μSR work,[15,16] the Néel temperatures of LaFeAsO$_{1-x}$F$_x$ with $x=0,0.03$ are 137 ± 3 and 120 ± 2 K, respectively. Figure 1(c) summarizes the structural and magnetic phase diagram determined from the present work. One of the key differences between the present phase diagram and that determined by μSR and Mössbauer-effect measurements[15] is the presence of the orthorhombic lattice distortion in underdoped superconducting LaFeAsO$_{1-x}$F$_x$. This indicates that the evolution from antiferromagnetism to superconductivity is not directly associated with the tetrago-
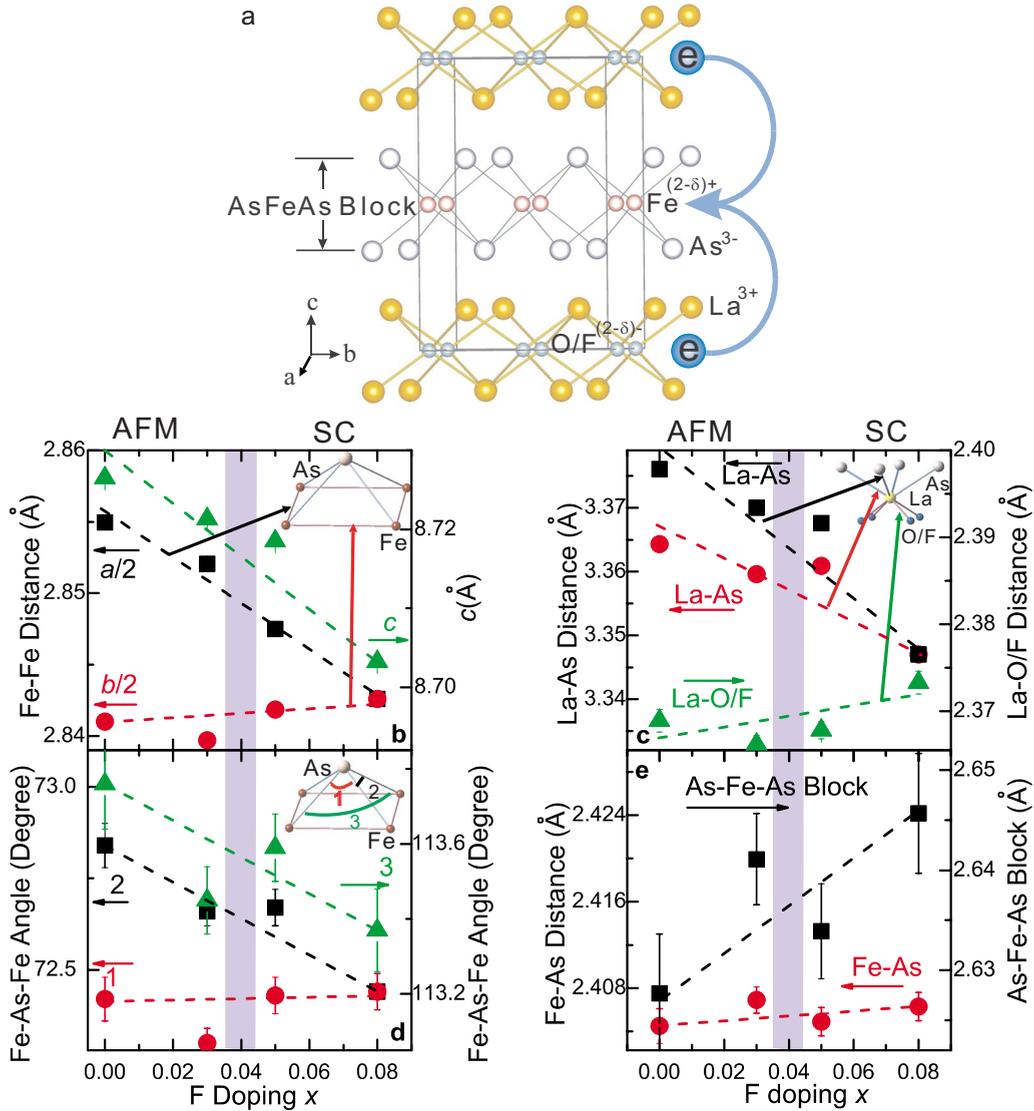
orthorhombic lattice distortion extends into the superconductivity dome in LaFeAsO$_{1-x}$F$_x$, similar to that of SmFeAsO$_{1-x}$F$_x$.[14]

To demonstrate this, we show in Fig. 2(a) a comparison of the high-resolution BT-1 data for LaFeAsO$_{1-x}$F$_x$ with $x=0,0.03,0.05$, and 0.08 taken at 4 K. While the parent compound LaFeAsO shows clear evidence of the orthorhombic lattice distortion as illustrated by the splitting of the $(4,0,0)_o$ and $(0,4,0)_o$ peaks, doping F gradually reduces the splitting of these peaks until they become a single resolution-limited peak corresponding to tetragonal symmetry for $x=0.08$.[7] For $x=0.03$, one can see a clear splitting of the $(4,0,0)_o$ and $(0,4,0)_o$ peaks. Although a well-resolved splitting is no longer observable in the $x=0.05$ sample, the peak width is broader than the resolution-limited case of $x=0.08$ [Fig. 2(a)]. In particular, we note that the width of the $(0,0,6)$ peak, which is not sensitive to the in-plane lattice distortion, is resolution limited for all concentrations. Hence the peak broadening for the in-plane peaks of the $x=0.05$ sample must arise from the underlying orthorhombic structure. In addition, we would expect that the temperature dependence of the $(2,2,0)_T$ reflection peak intensity (not integrated intensity) measured by the high-resolution BT-1 should decrease

FIG. 4. (Color online) Low temperature structural evolution of LaFeAsO$_{1-x}$F$_x$ as a function of F doping obtained from analysis of the BT-1 data. There is no sudden structural transition as the AFM order is replaced by the superconducting phase. The atomic positions of LaFeAsO$_{1-x}$F$_x$ and their temperature dependence are shown in Tables I and II. (a) schematic defining the As-Fe-As block and illustrating the process of electron doping. (b) a, b, c lattice constants of the orthorhombic unit cell and the two Fe-Fe nearest-neighbor distances as a function of F doping. Similar to CeFeAsO$_{1-x}$F$_x$, F doping only suppresses the long axis of the orthorhombic structure. (c) La-O/F and La-As distances as a function of F doping. The slight increase in the La-O/F block size is compensated by a much larger reduction in the La-As distance, resulting in an overall c-axis lattice contraction as shown in (b). (d) Fe-As-Fe bond angles as defined in the inset versus F doping. While angle 1 hardly changes with doping, angles 2 and 3 decrease substantially with increasing F doping. (e) The Fe-As bond distance and As-Fe-As block size versus F doping. The Fe-As distance is independent of F doping.

nal to orthorhombic structural phase transition. Instead, our data appear to support the idea that commensurate AFM order is a competing ground state to superconductivity, much like the case of electron-doped high-T_c copper oxides.[18,19] Theoretically, it has been argued that the orthorhombic lattice distortion in RFeAsO$_{1-x}$F$_x$ is associated with nematic ordering of the Fe spin fluctuations and therefore is a precursor of long-range AFM order.[20–22]

Previous systematic work on CeFeAsO$_{1-x}$F$_x$ (Ref. 8) found that the impact of F doping is to compress the c and a axes of the orthorhombic structure, where $c > a > b$, while leaving the b axis unchanged. The decrease in the c-axis lattice constant is mostly due to the distance reduction of the CeO and FeAs blocks. To see if this is also true for LaFeAsO$_{1-x}$F$_x$, we plot the doping dependence of the Fe-Fe distance [Fig. 4(b)], La-As and La-O/F distances [Fig. 4(c)], Fe-As-Fe bond angles [Fig. 4(d)], and Fe-As/As-Fe-As block distances [Fig. 4(e)] obtained from detailed analysis of the high-resolution BT-1 data (see Tables I and II for details). Consistent with earlier work on CeFeAsO$_{1-x}$F$_x$,[8] we find that electron doping suppresses the long a axis of the orthorhombic structure while leaving the short b axis unchanged. Similarly, doping electrons reduces the distance between the LaO and FeAs blocks, mostly likely due to increased Coulomb attraction between these two blocks. Since the Fe-As distance (2.404 Å) is essentially doping independent [Fig.

TABLE II. Refined crystal structure parameters of LaFeAsO$_{1-x}$F$_x$ with $x=0,0.03,0.05$ at 2 K. Space group: *Cmma*. Atomic positions: La: $4g(0,\frac{1}{4},z)$; Fe: $[4b(\frac{1}{4},0,\frac{1}{2})]$; As: $4g(0,\frac{1}{4},z)$; and O/F: $4a(\frac{1}{4},0,0)$.

Atom		$x=0$	$x=0.03$	$x=0.05$
	a(Å)	5.70988(9)	5.70407(8)	5.6995(2)
	b(Å)	5.68195(9)	5.67936(8)	5.6837(2)
	c(Å)	8.7265(1)	8.7213(1)	8.7185(1)
La	z	0.1430(3)	0.1427(2)	0.1431(2)
As	z	0.6506(3)	0.6514(3)	0.6510(3)
	R_p(%)	4.26	4.36	5.21
	w_{Rp}(%)	5.47	5.75	6.87
	χ^2	1.005	0.9327	1.221

4(e)], the net effect of the a-axis lattice contraction is to push the diagonal Fe-As-Fe angle toward the ideal value of 109.47° for the perfect FeAs tetrahedron [Fig. 4(d)]. The lattice structure is seen to evolve smoothly across the AFM to superconductivity phase transition. These results confirm the notion that the most effective way to increase T_C in Fe-based superconductors is to decrease the deviation of the Fe-As(P)-Fe bond angle from the ideal FeAs tetrahedron.[8,23]

III. CONCLUSIONS

In summary, we have shown that the orthorhombic lattice distortion present in undoped LaFeAsO can extend beyond the AFM to superconductivity phase boundary, whereas the static long-range AFM ordered phase does not seem to coexist with superconductivity. The phase diagram of electron-doped LaFeAsO$_{1-x}$F$_x$ can therefore be sketched as in Fig. 1(c), showing clear coexistence of superconductivity with either the orthorhombic or tetragonal lattice structure.

ACKNOWLEDGMENTS

*daip@ornl.gov

[1] Y. Kamihara, T. Watanabe, M. Hirano, and H. Hosono, J. Am. Chem. Soc. **130**, 3296 (2008).

[2] X. H. Chen, T. Wu, G. Wu, R. H. Liu, H. Chen, and D. F. Fang, Nature (London) **453**, 761 (2008).

[3] G. F. Chen, Z. Li, D. Wu, G. Li, W. Z. Hu, J. Dong, P. Zheng, J. L. Luo, and N. L. Wang, Phys. Rev. Lett. **100**, 247002 (2008).

[4] Zhi-An Ren, G. Che, X. Dong, J. Yang, W. Lu, W. Yi, X. Shen, Z. Li, L. Sun, F. Zhou, and Z. X. Zhao, Europhys. Lett. **83**, 17002 (2008).

[5] H. H. Wen, G. Mu, L. Fang, H. Yang, and X. Zhu, Europhys. Lett. **82**, 17009 (2008).

[6] G. F. Chen, Z. Li, G. Li, J. Zhou, D. Wu, J. Dong, W. Z. Hu, P. Zheng, Z. J. Chen, H. Q. Yuan, J. Singleton, J. L. Luo, and N. L. Wang, Phys. Rev. Lett. **101**, 057007 (2008).

[7] C. de la Cruz, Q. Huang, J. W. Lynn, J. Li, W. Ratcliff II, J. L. Zarestky, H. A. Mook, G. F. Chen, J. L. Luo, N. L. Wang, and Pengcheng Dai, Nature (London) **453**, 899 (2008).

[8] Jun Zhao, Q. Huang, C. de la Cruz, Shiliang Li, J. W. Lynn, Y. Chen, M. A. Green, G. F. Chen, G. Li, Z. Li, J. L. Luo, N. L. Wang, and Pengcheng Dai, arXiv:0806.2528 (unpublished).

[9] Q. Huang, Y. Qiu, Wei Bao, J. W. Lynn, M. A. Green, Y. Chen, T. Wu, G. Wu, and X. H. Chen, arXiv:0806.2776 (unpublished).

[10] A. I. Goldman, D. N. Argyriou, B. Ouladdiaf, T. Chatterji, A. Kreyssig, S. Nandi, N. Ni, S. L. Bud'ko, P. C. Canfield, and R. J. McQueeney, arXiv:0807.1525 (unpublished).

[11] M. A. McGuire, A. D. Christianson, A. S. Sefat, B. C. Sales, M. D. Lumsden, R. Jin, E. A. Payzant, D. Mandrus, Y. Luan, V. Keppens, V. Varadarajan, J. W. Brill, R. P. Hermann, M. T. Sougrati, F. Grandjean, and G. J. Long, arXiv:0806.3878 (unpublished).

[12] Y. Chen, J. W. Lynn, J. Li, G. Li, G. F. Chen, J. L. Luo, N. L. Wang, Pengcheng Dai, C. dela Cruz, and H. A. Mook, Phys. Rev. B **78**, 064515 (2008).

[13] Jun Zhao, W. Ratcliff II, J. W. Lynn, G. F. Chen, J. L. Luo, N. L. Wang, J. Hu, and Pengcheng Dai, arXiv:0807.1077 (unpublished).

[14] S. Margadonna, Y. Takabayashi, M. T. McDonald, M. Brunelli, G. Wu, R. H. Liu, X. H. Chen, and K. Prassides, arXiv:0806.3962 (unpublished).

[15] H. Luetkens, H.-H. Klauss, M. Kraken, F. J. Litterst, T. Dellmann, R. Klingeler, C. Hess, R. Khasanov, A. Amato, C. Baines, J. Hamann-Borrero, N. Leps, A. Kondrat, G. Behr, J. Werner, and B. Buechner, arXiv:0806.3533 (unpublished).

[16] J. P. Carlo, Y. J. Uemura, T. Goko, G. J. MacDougall, J. A. Rodriguez, W. Yu, G. M. Luke, Pengcheng Dai, N. Shannon, S. Miyasaka, S. Suzuki, S. Tajima, G. F. Chen, W. Z. Hu, J. L. Luo, and N. L. Wang, arXiv:0805.2186 (unpublished).

[17] In a recent μSR work, S. Takeshita, R. Kadono, M. Hiraishi, M. Miyazaki, A. Koda, Y. Kamihara, and H. Hosono, arXiv:0806.4798 (unpublished), suggest that weak spin-glass-like magnetism coexists with superconductivity in a LaFeAsO$_{1-x}$F$_x$ $x=0.06$ sample. Since neutron measurements present here are sensitive only to static long-range order, our data do not eliminate the possibility of short-range, spin-glass-like, magnetic correlations coexisting with superconductivity.

[18] H. J. Kang, P. Dai, H. A. Mook, D. N. Argyriou, V. Sikolenko, J. W. Lynn, Y. Kurita, S. Komiya, and Y. Ando, Phys. Rev. B **71**, 214512 (2005).

[19] S. D. Wilson, Shiliang Li, Jun Zhao, G. Mu, Hai-hu Wen, Jeffrey W. Lynn, Paul G. Freeman, Louis-Pierre Regnault, Klaus

Habicht, and Pengcheng Dai, Proc. Natl. Acad. Sci. U.S.A. **104**, 15259 (2007).

[20] C. Fang, H. Yao, W.-F. Tsai, J. P. Hu, and S. A. Kivelson, Phys. Rev. B **77**, 224509 (2008).

[21] C. Xu, M. Müller, and S. Sachdev, Phys. Rev. B **78**, 020501(R)

(2008).

[22] C. Xu, Y. Qi, and S. Sachdev, arXiv:0807.1542 (unpublished).

[23] C. H. Lee, A. Iyo, H. Eisaki, H. Kito, M. T. Fernandez-Diaz, T. Ito, K. Kihou, H. Matsuhata, M. Braden, and K. Yamada, J. Phys. Soc. Jpn. **77**, 083704 (2008).